Research Article

A Secreted Form of ADAM9 Promotes Carcinoma Invasion through Tumor-Stromal Interactions

Antonio Mazzocca,[1,4] Roberto Coppari,[2] Raffaella De Franco,[4] Je-Yoel Cho,[3] Towia A. Libermann,[3] Massimo Pinzani,[4] and Alex Toker[1]

Departments of [1]Pathology and [2]Medicine and [3]Genomics Center, Beth Israel Deaconess Medical Center, Harvard Medical School, Boston, Massachusetts and [4]Dipartimento di Medicina Interna, Centro di Ricerca, Trasferimento e Alta Formazione MCIDNENT, University of Florence, Florence, Italy

Abstract

Tumor cell invasion is a process regulated by integrins, matrix-degrading enzymes, and interactions with host tissue stromal cells. The ADAM family of proteins plays an important role in modulating various cellular responses. Here, we show that an alternatively spliced variant of ADAM9 is secreted by hepatic stellate cells and promotes carcinoma invasion. ADAM9-S induced a highly invasive phenotype in several human tumor cell lines in Matrigel assays, and the protease activity of ADAM9-S was required for invasion. ADAM9-S binds directly to $\alpha_6\beta_4$ and $\alpha_2\beta_1$ integrins on the surface of colon carcinoma cells through the disintegrin domain. ADAM9-S was also able to cleave laminin and promote invasion. Analysis of human liver metastases revealed that ADAM9 is expressed by stromal liver myofibroblasts, particularly those that are localized within the tumor stroma at the invasive front. These results emphasize the importance of tumor-stromal interactions in invasion and suggest that ADAM9-S can be an important determinant in the ability of cancer cells to invade and colonize the liver. (Cancer Res 2005; 65(11): 4728-38)

Introduction

The process of tumor cell invasion and metastasis is conventionally understood as the migration of tumor cells that detach from the primary tumor, enter lymphatic vessels or the bloodstream, and seed in distant organs (1). Tumor cell invasion is a process regulated by integrins, matrix-degrading enzymes, and cell-cell interactions with host tissue stromal cells and cell-matrix interactions with components of the extracellular matrix (ECM). Thus, during the invasive process, tumor-stromal interactions are essential for inducing tissue remodeling and promoting tumor cell migration across the ECM barrier at both primary and metastatic sites (2).

The liver is a preferential site of metastasis from a variety of tumors, such as colon cancer, breast carcinoma, and melanoma (3). In liver metastasis, the local host stroma, a complex mixture of fibroblasts, myofibroblasts, endothelial cells, and inflammatory cells, is considered to play a crucial role in the infiltration and colonization of the organ by metastatic cells, such that the outcome of metastasis depends on multiple interactions of metastatic cells with the stromal cells in the liver microenvironment (4). Morphologic evidence suggest that hepatic stellate cells (HSC) contribute to the genesis of myofibroblasts surrounding colorectal liver metastases (5, 6). HSCs are multifunctional liver mesenchymal cells residing around the endothelial cells in the space of Disse. Following acute or chronic liver tissue injury, HSCs undergo a process of activation toward a myofibroblast-like phenotype characterized by increased proliferation, motility, contractility, and synthesis of ECM components and matrix-degrading enzymes (7). HSCs become activated when exposed to soluble factors released by melanoma cells and, in turn, release factors, which directly influence cancer cell motility (8). Consequently, it has been proposed that HSCs may contribute to the development of the metastatic stroma and also influence the local invasion of metastatic cells. However, the mechanisms underlying this process remain largely undefined.

The ability of tumor cells to invade and colonize different tissues depends on their ability to remodel the host tissue ECM, a process attributed to the secretion of a variety of proteases from both tumor cells and activated stromal cells (9). The proteolytic modification of the ECM by metalloproteases allows malignant cells to locally invade and form distant metastases (10). The demonstration of the tumor-stroma interdependence is provided by the fact that most of the proteolytic enzymes localized at the invasive front are produced by host stromal cells and not by the invading tumor (11–14). The ADAM family of proteins is a group of metalloproteases that belong to the zinc protease superfamily. ADAMs are transmembrane proteins that contain both disintegrin and metalloprotease domains and therefore have both cell adhesive and protease activities (15, 16). Thus, ADAMs have the potential to be key modulators of cell-matrix interactions through the activities of their constituent domains. Previous studies have suggested a role for the ADAM proteins in regulating tumor progression. For example, ADAM15 binds to $\alpha_v\beta_3$-expressing melanoma cells (17), whereas ADAM12 binds to several cancer cell lines through cysteine-rich domain-syndecan interactions (18). ADAM9 has been shown to bind to $\alpha_6\beta_1$-expressing fibrosarcoma cells through an integrin-binding motif leading to a marked induction of cell motility (19). ADAM9 (also known as meltrin γ or metalloprotease disintegrin cysteine-rich protein-9) is an 84-kDa, membrane-anchored cell surface protein widely expressed in human tissues (20). The metalloprotease domain of ADAM9 has been implicated in ectodomain shedding of membrane-anchored heparin-binding epidermal growth factor–like growth factor (20) and may also have proteolytic activity toward ECM proteins (21). Despite these observations, the role of ADAM9 in cancer progression has not been explored. However, it was recently reported that in breast carcinoma increased expression of ADAM9 correlates with cancer progression (22) and elevated mRNA levels of both ADAM9 and

Note: Supplementary data for this article are available at Cancer Research Online (http://cancerres.aacrjournals.org/).

J-Y. Cho is currently at the Department of Biochemistry, School of Dentistry, Kyungpook National University (Daegu, South Korea).

Requests for reprints: Alex Toker, Department of Pathology, Beth Israel Deaconess Medical Center, Harvard Medical School, 330 Brookline Avenue, RN-237, Boston, MA 02215. Phone: 617-667-8535; Fax: 617-667-3616; E-mail: atoker@bidmc.harvard.edu.

©2005 American Association for Cancer Research.

ADAM12 have been found in liver metastases from colon carcinomas (23). Moreover, overexpression of ADAM9 in non–small cell lung cancer correlates with metastasis to the brain (24).

In this study, we employed activated stromal liver myofibroblasts to study tumor-stromal interactions during invasion of carcinoma cells, which preferentially metastasize to the liver. We found that a soluble form of ADAM9 secreted by activated HSCs induces colon carcinoma cell invasion *in vitro* and that this requires both protease activity and binding to the $\alpha_6\beta_4$ and $\alpha_2\beta_1$ integrins.

Materials and Methods

Materials. Murine Engelbreth-Holm-Swarm (EHS) laminin-1 purified from basement membrane of EHS sarcoma was purchased from Sigma Chemical Co. (St. Louis, MO). Matrigel was from Collaborative Biomedical Products (Bedford, MA); Iscove's medium and DMEM were from Invitrogen (Carlsbad, CA). All other chemicals were laboratory reagent grade.

Cell culture. WRL68, HepG2, MCF-7, clone A, and MDA-MB-231 cell lines were obtained from American Type Culture Collection (Manassas, VA) and maintained in DMEM or RPMI (clone A) supplemented with 10% fetal bovine serum. OMM2.3 cells were grown in RPMI.

Isolation of hepatic stellate cells. Human HSCs were isolated from wedge sections of normal human liver unsuitable for transplantation as described previously (25). Cells were cultured in Iscove's modified DMEM supplemented with insulin, glutamine, and 20% fetal bovine serum.

Microscopy. Cells were plated on glass coverslips in the presence of serum-containing medium, fixed with 2% paraformaldehyde, and permeabilized with 1% Triton X-100. Coverslips were blocked with 20% heat-inactivated normal goat serum and incubated with TRITC-phalloidin (Molecular Probes, Eugene, OR, Invitrogen). Staining was visualized by confocal scanning laser microscopy (MRC-1024, Bio-Rad Laboratories, Hercules, CA).

Fast protein liquid chromatography. Conditioned medium (CM, 2 L) was collected, filtered through a 0.22 μm filter, and concentrated 50-fold using a Vivaflow 70 5-kDa mass cutoff (Sartorius, Edgewood, NY). The concentrate was applied to Superose 12 HR10/30 column (Amersham, Piscataway, NJ) equilibrated with 50 mmol/L Tris-HCl (pH 7.5). The column was eluted at 0.4 mL/min, and 0.5 mL fractions were collected, dialyzed, and assayed for Matrigel invasion activity. The peak was pooled, applied to a UNO Q1 anion exchange chromatography column (Bio-Rad Laboratories), and chromatographed with a linear gradient of 0 to 0.6 mol/L NaCl, 1.0 mL/min.

Mass spectrometry. Mass analysis was done using the Ciphergen SELDI Protein Biology System II (Ciphergen Biosystems, Inc., Fremont, CA). Protein bands excised from SDS polyacrylamide gels were subjected to in-gel digestion with trypsin, and resulting peptides were spotted on a SELDI ProteinChip array with a hydrophobic surface. The spots were washed with 10% acetonitrile and 5 mg/mL (α-cyano-4-hydroxy cinnamic acid) in 50% acetonitrile, and 0.5% trifluoroacetic acid was added to the surfaces. Mass identification was made by averaging 150 shots in Ciphergen Biosystems Protein Biology System II. Proteins were identified by searching the publicly available National Center for Biotechnology Information database.

Matrigel chemoinvasion assay. Matrigel chemoinvasion assays were carried out essentially as described previously using chemotaxis chambers (Neuro Probe, Inc., Gaithersburg, MD) with 8 μm pore filters (Nucleopore, Millipore Corp., Billerica, MA; ref. 26). Briefly, filters were coated with Matrigel and cells were added to the upper chamber. HSC-CM, chromatography fractions, purified recombinant ADAM9-S (20 μg/mL), or NIH3T3-CM (control) were applied to lower chamber. Assays were carried out for 12 hours, after which cells on the upper surface of the filter were removed and filter stained with crystal violet. Cells on the bottom side of the filter were counted. For invasion on laminin, filters were coated with 20 μg/mL EHS laminin-1.

RNA isolation and PCR. Total RNA from human HSCs was isolated with TRIzol (Life Technologies, Carlsbad, CA, Invitrogen). After reverse transcription of 500 ng total RNA by oligo(dT) priming, the resulting single-stranded cDNA was used for amplifying ADAM9-S by PCR using the following oligonucleotides: sense 5′-GCGGGATCCACGCCGAGATGGGGTCTGGCGCG-3′ and antisense 5′-CTCGAGAAATTTCAGTGACAGCCCAGTGGCACA-3′. The amplified fragment was subcloned into the pcDNA4/TO/Myc-His A vector (Invitrogen) and verified by sequencing.

Transient transfection. Cells were transiently transfected with ADAM9-S or vector alone control using the LipofectAMINE reagent (Life Technologies, Invitrogen) according to the manufacturer's directions. After 24 hours, cells were resuspended in serum-free medium containing 0.1% bovine serum albumin (BSA) and used for chemoinvasion assays.

Cell proliferation assay. Cells were seeded at 5×10^3 per well in 96-well plates. HSC-CM or control medium was added after 12 hours at day 0. HSC-CM was changed every 48 hours and growth was assessed using the 3-(4,5-dimethylthiazol-2-yl)-5-(3-carboxymethoxyphenyl)-2-(4-sulphophenyl)-2H-tetrazolium, inner salt proliferation assay (Promega Corp., Madison, WI).

Flow cytometry analysis. For flow cytometry analysis, clone A cells were trypsinized, harvested, and washed with in DMEM. Cells were preincubated with human recombinant ADAM9-S (R&D Systems, Inc., Minneapolis, MN) for 30 minutes. Primary monoclonal antibodies (mAb; anti-α_2: HAS3, anti-α_6: 2B7, anti-β_1: mAb13, and anti-β_4: 3E1) were bound to cells, after which cells were washed and incubated with goat anti-mouse FITC. Fluorescence was analyzed using a FACScan flow cytometer (Beckman Coulter, Inc., Fullerton, CA).

Adhesion assay. Cell adhesion assays to recombinant ADAM9-S were carried out in 96-well plates, which were precoated with 10 μg/mL ADAM9-S. Nonspecific sites were blocked with 2% BSA. Before binding, cells were preincubated with anti-integrin antibodies (α_2: P1E6, α_3: P1B5, α_5: mAb16, α_6: α_6: GoH3, β_1: mAb13, and β_4: 3E1) at a final concentration of 10 μg/mL in PBS containing 1 mmol/L $CaCl_2$, 1 mmol/L $MgCl_2$, and 0.5 mmol/L $MnCl_2$. After 1 hour at 37°C, 0.2% glutaraldehyde (100 μL) in PBS was added, and bound cells were fixed. Nonadherent cells were removed by washing in PBS. Cell adhesion was determined by staining with crystal violet and quantified by measuring absorbance at 595 nm.

Protein immunoblotting, immunoprecipitation, and zymography. For immunoblot analysis, cells were lysed in lysis buffer [50 mmol/L Tris-HCl (pH 7.4), 1% Igepal, 150 mmol/L NaCl, 5 mmol/L EDTA (pH 7.4)] and protease inhibitor cocktail (Sigma-Aldrich). Proteins were separated by 10% SDS-PAGE and transferred to nitrocellulose membranes and ADAM9 was detected with an anti-ADAM9 polyclonal antibody (2 μg/mL, Chemicon, Temecula, CA). For immunoprecipitation, clone A cells were lysed with lysis buffer, and lysates were incubated with anti-integrin antibodies [anti-α_2: CD49b (Chemicon), anti-α_3: P1B5 (Chemicon), anti-α_5: P1D6 (Chemicon), anti-α_6: GoH3 (Beckman Coulter), anti-β_1: N29 (Chemicon), and β_4: 3E1 (Chemicon)] and protein G-agarose. Immunoprecipitates were separated on SDS-PAGE, transferred to nitrocellulose, and immunoblotted. For zymography, purified ADAM9-S was resolved under native conditions on 10% SDS-PAGE with 1 mg/mL gelatin and gelatinolytic activity was detected as described previously (27). For laminin zymography, human recombinant ADAM9-S (1 μg) was resolved on 10% SDS-PAGE under nonreducing conditions, containing 0.5 mg/mL laminin-1. Gels were washed thrice with 2.5% Triton X-100 and once with a buffer consisting of 20 mmol/L Tris-HCl, 500 mmol/L NaCl, 5 mmol/L $CaCl_2$, and 0.5 mmol/L $ZnCl_2$ (pH 7.4). Where indicated, 1,10-phenanthroline (100 μmol/L) was added during zymography. Gels were incubated overnight, stained with Coomassie blue, and destained with water.

Immunohistochemistry. Liver tissues were obtained from 19 patients who had undergone resection for liver metastases from colorectal tumors and from 4 patients affected by uveal melanoma who had undergone liver biopsy. Informed consent was obtained from all patients before the procedures and the study was approved by the Institutional Ethical Committee. Tissue sections were taken from the interface between the tumor and the adjacent liver (junctional specimen) as well as from liver at distance from the tumor (distant normal specimen). In the junctional specimens, four distinct areas were examined: (*a*) the tumor; (*b*) the capsule, if present; (*c*) the junction between tumor and adjacent liver (arbitrarily defined as between the interface of tumor-liver or capsule-liver and 2 mm away from this junction); and (*d*) close "normal" liver defined as the region between 2 and 4 mm from the tumor-liver or capsule-liver

interface. Tissue sections were collected onto glass slides, fixed, and incubated sequentially with anti-ADAM9 antibody (50 μg/mL) followed by incubation with the alkaline phosphate anti-alkaline phosphatase complex as described (28). Activated HSCs were detected with anti–smooth muscle actin (SMA; clone 1A4, Sigma Chemical).

Statistical analysis. Data were analyzed using the unpaired *t* test. $P = 0.05$ was considered statistically significant.

Results

Activated hepatic stellate cells promote Matrigel chemoinvasion. We first evaluated the ability of rat liver and spleen extracts to stimulate invasion through Matrigel *in vitro*. Liver extracts induced a 3-fold increase in invasion of clone A (colon carcinoma), MDA-MB-231 (breast carcinoma), and OMM2.3 (uveal melanoma) cells when compared with spleen extracts or control (Fig. 1*A*). Therefore, the liver contains significant migration and invasion-promoting activities for cells that are derived from tissues that preferentially metastasize to the liver. CM collected from activated human HSCs also potently induced carcinoma invasion of these cells lines (Fig. 1*A*). Conversely, medium collected from the nontransformed hepatocyte-derived cell line WRL68 did not promote invasion. The ability of HSC-CM to induce cell proliferation was also evaluated, but no significant differences in growth were observed when compared with control (Fig. 1*B*). HSC-CM induced a 10-fold increase in clone A invasion compared with medium collected from quiescent HSCs (Fig. 1*C*). Although increasing concentrations of HSC-CM stimulated Matrigel chemoinvasion, a classic bell-shaped concentration curve was not observed, suggesting that soluble factors released by activated HSCs do not function as classic chemoattractants.

We next tested the effect of CM from quiescent and activated HSCs on carcinoma cell morphology. Clone A cells treated with CM from activated HSCs showed a motile scattered morphology with spread cells projecting filopodia and lamellapodia (Fig. 1*D*). Conversely, cells treated with CM from quiescent HSCs retained the conserved epithelial morphology similar to those treated with control medium. In tumor cells, actin polymerization is required for filopodia and lamellapodia formation, which are in turn needed for invasion (29). Clone A cells treated with wither serum-free medium or CM collected from quiescent HSCs showed F-actin staining in stress fibers, whereas cells treated with CM from activated HSCs revealed intense F-actin staining in the periphery of the cells and a

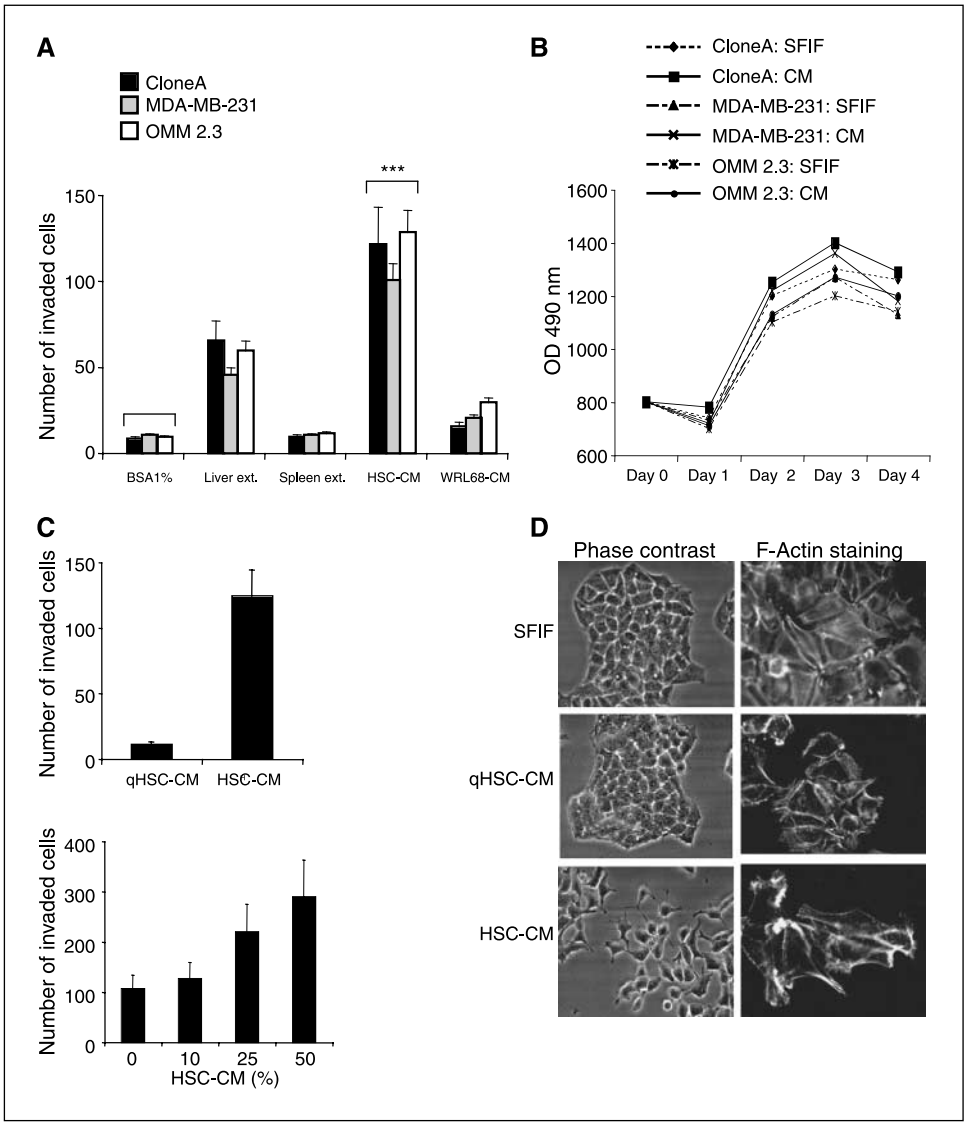

Figure 1. Soluble factors released by activated HSCs promote carcinoma invasion. *A,* clone A, MDA-MB-231, and OMM2.3 cells were assayed for their ability to invade Matrigel toward control BSA (1%), liver and spleen extracts, and CM from HSCs and WRL68 cells. ***, $P < 0.001$. *B,* growth curves of clone A, MDA-MB-231, and OMM2.3 cells incubated over a 4-day period with either HSC-CM or control medium [serum-free, insulin-free (*SFIF*) medium]. *C,* clone A cells were assayed by Matrigel chemoinvasion with CM from quiescent (*qHSC-CM*) and activated (*HSC-CM*) cells (*left*) or with HSC-CM concentrated 10-fold by ultrafiltration and added to a lower compartment of the chamber at the indicated concentrations (*right*). All experiments were carried out in triplicate. *Bars,* SD. *D,* morphology of clone A cells incubated for 6 hours with CM collected from quiescent and activated HSC and with control SFIF medium. *Left,* phase-contrast images (magnification, ×100); *right,* F-actin polymerization as revealed by TRITC-phalloidin staining (magnification, ×200).

redistribution of F-actin toward the leading edge (Fig. 1*D*). These data show that soluble factor(s) released by activated HSCs induces an aggressive invasive phenotype in carcinoma cells.

Identification of ADAM9-S. To identify the soluble factor(s) released by activated HSCs capable of promoting carcinoma invasion, we fractionated HSC-CM on fast protein liquid chromatography using gel filtration and anion exchange chromatography. The resulting fractions were assayed for their ability to induce carcinoma invasion in the Matrigel assay (Supplementary Figs. S1A and S1B). The peak active fractions were resolved by SDS PAGE and silver stained, and a single protein band at 55 kDa directly correlated with invasion-promoting activity (Supplementary Fig. S1C). The 55-kDa band was excised from a parallel, unstained gel and subjected to in-gel digestion with trypsin. The resulting peptides were analyzed by surface laser-enhanced desorption ionization-time of flight mass spectrometry. A protein-free gel digest was also run in parallel to identify signals associated with autolysis of the trypsin and potential proteolytic fragments of contaminant proteins (Fig. 2*A*). A total of 17 unique peptides were used for a ProFound search of human protein sequences between 0 and 150 kDa (Fig. 2*B*). Each peptide sequence was used to search the publicly available SwissPROT and TrEMBL databases using the IdenTag search algorithm and consistently returned the secreted form of the ADAM9 (ADAM9-S) protein as exactly matching the peptide sequences obtained in mass spectrometry analysis.

Activated hepatic stellate cells express ADAM9. The above results suggest that ADAM9-S, secreted by activated HSCs, could promote carcinoma invasion. To test this hypothesis, Matrigel invasion assays were carried out using purified ADAM9-S. Purified ADAM9-S and HSC-CM potently induced chemoinvasion of clone A and MDA-MB-231 cells (Fig. 3*A*; data not shown). Moreover, this activity was blocked when ADAM9-S was immunodepleted with a specific anti-ADAM9 antibody but not with control IgG. Immunodepletion of HSC-CM with anti-ADAM9 did not completely eliminate invasion, suggesting the presence of soluble factors distinct from ADAM9-S released by HSCs, which are also able to promote invasion (Fig. 3*A*).

To investigate the expression of ADAM9-S during the activation of HSCs, immunoblotting was done on total cell lysates and culture medium obtained from 2-day-old quiescent cells and from two distinct passages of the same culture of activated HSCs (Fig. 3*B*). This analysis revealed that the expression of ADAM9-S occurred during the transition from a quiescent state to an activated state, as no ADAM9-S expression could be detected in freshly isolated, quiescent HSCs. In addition, neither hepatocyte-derived cell lines (WRL68 and HepG2) nor noninvasive carcinoma cells (MCF-10A and Caco-2) revealed any detectable ADAM9-S expression (Fig. 3*B*). Interestingly, we also detected expression of the longer ADAM9-L variant in activated HSCs as well as the pro-ADAM9-L form, which includes the prodomain (Fig. 3*B*).

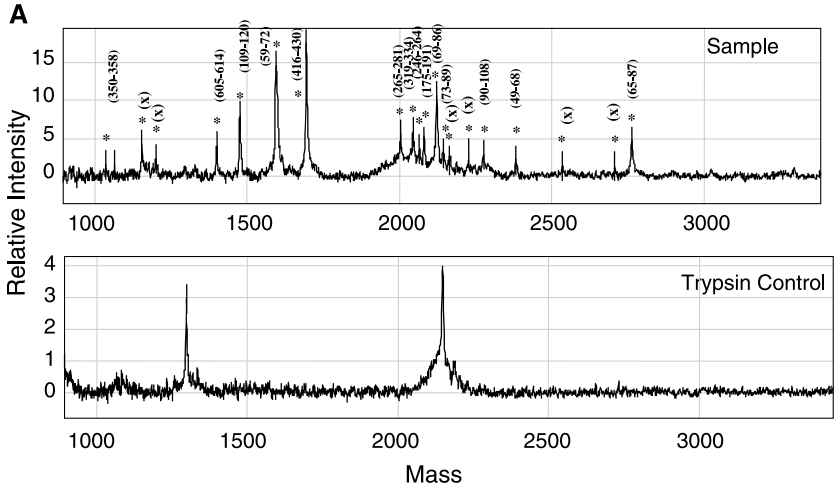

B

ADAM9 identification by peptide mass fingerprint used for database queries.

Matched mass	Computed mass	Peptide sequence of ADAM9-S (55-kDA)	Cut	Residues	
Trypsin digested					
1034.820	1034.247	FLPGGTLCR	0	350	358
1399.190	1398.587	DQLWRSYFRK	2	605	614
1474.700	1473.654	YDMMGRNQTAVR	1	109	120
1593. 570	1592.791	CGVSNKDIEKETAK	2	59	72
1692.480	1691.969	AKAAPKDCFIEVNSK	2	416	430
2003.010	2002.193	EEEEPPSMTQLLRRR	2	73	88
2003.010	2004.205	FSSCSAEDFEKLTLNK	1	265	281
2043.070	2042.364	CELDPCCESTCKLK	1	319	334
2064.640	2063.302	CSCGAKSIMNSGASGSR	1	246	264
2064.640	2066.175	RSQTYESDGKNQANPSR	3	615	632
2080.150	2081.496	LITRRRHDSAQLVLKK	4	175	191
2120.700	2119.291	TAKDEEEEPPSMTQLLR	1	69	86
2142.070	2142.381	DEEEEPPSMTQLLRRR	3	73	89
2275.260	2275.677	AVLPQTRYVELFIVVDKER	2	90	108
2275.260	2275.479	KDEEEEPPSMTQLLRR	2	69	87
2380.720	2382.741	DVYKEPLKCGVSNKDIEK	3	49	68
2760.220	2761.016	TAKDEEEEPPSMTQLLRR	3	65	87

Figure 2. Identification of ADAM9-S. *A,* surface laser-enhanced desorption ionization-time of flight mass spectrum showing isotopic resolution of the peptides obtained from the in-gel digestion of the 55-kDa band shown in Supplementary Fig. S1 (*top*) and of a protein-free sample processed in parallel (trypsin control, *bottom*). Based on the internally calibrated peptide masses derived from the spectrum, the protein was identified as ADAM9-S. Tryptic fragment masses unique to the ADAM9-S band are labeled with *asterisks*. The residues covered by the identified fragments are indicated in *parentheses*. Unidentified fragments are denoted by *x*. *B,* mass spectrometry fingerprint obtained from the peptides in *A*, showing the matched and computed masses obtained by the spectrum and the peptide sequences corresponding to ADAM9-S.

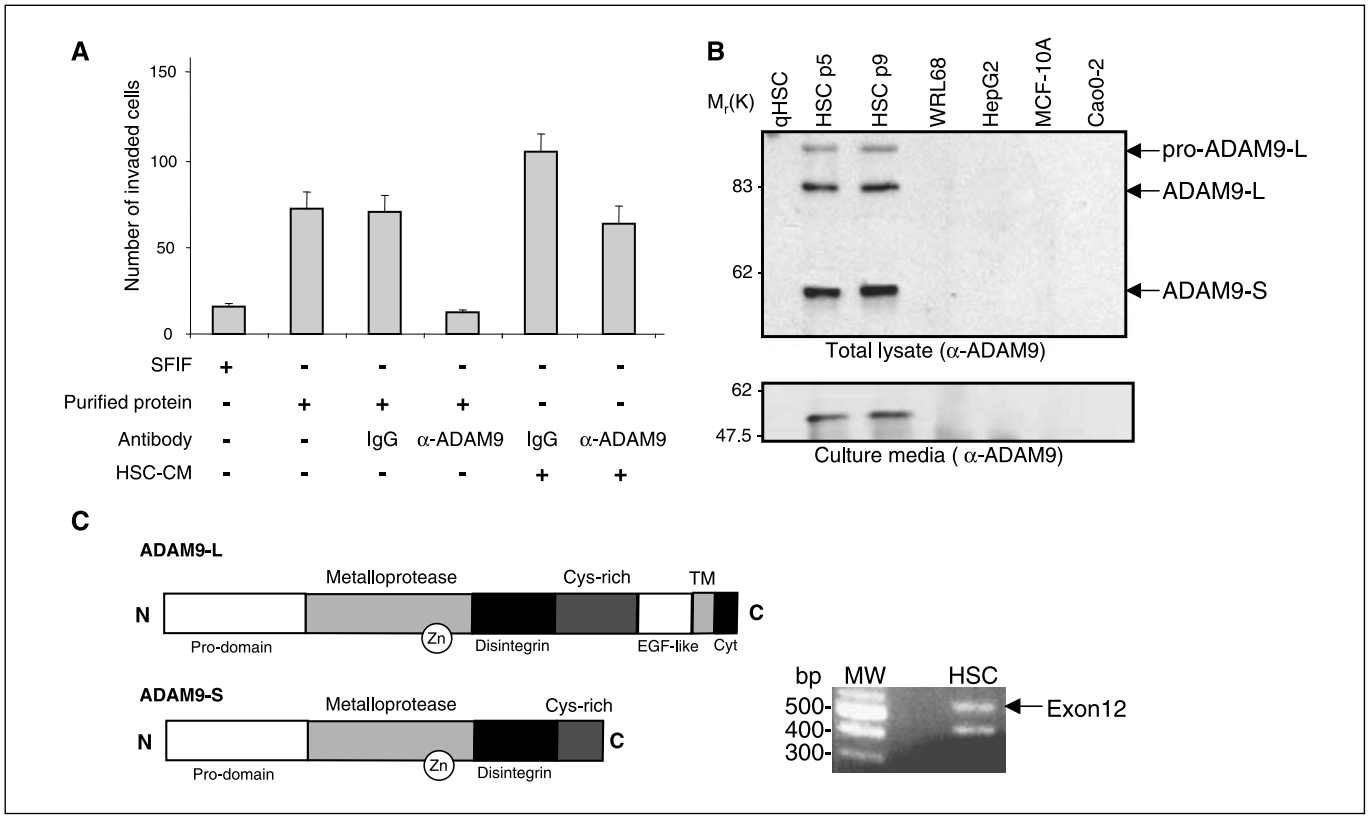

Figure 3. Identification of ADAM9 secreted by HSCs. *A,* Matrigel invasion assay of clone A cancer cells using purified ADAM9-S or HSC-CM alone or immunodepleted with anti-ADAM9 antibody as indicated. SFIF and control IgG were used as negative controls. *B,* immunoblot analysis of ADAM9-S and ADAM9-L in total cell lysates (*top*) and culture medium (*bottom*) of quiescent (*qHSC*) and activated HSCs (*aHSC*) after 5 (*p5*) and 9 (*p9*) serial passages and from WRL68, HepG2, MCF-10A, and Caco-2 cells. *C,* domain structure of the long (*ADAM9-L*) and short (*ADAM9-S*) forms of ADAM9, and evaluation of the presence of exon 12, by RT-PCR. The 500-bp band represents a PCR product inclusive of exon 12 in ADAM9-S, whereas the smaller 400-bp fragment represents a PCR product lacking exon 12 from the ADAM9-L message.

ADAM9 was originally cloned as an 84-kDa transmembrane protein comprising 819 amino acids with a characteristic domain structure, which include a prodomain, a metalloproteinase domain, a disintegrin-like region, a cysteine-rich domain, an epidermal growth factor–like domain, a transmembrane domain, and an intracellular tail (Fig. 3*C*; ref. 20). Analysis of the human genome map in the Celera database (30) revealed the presence of an additional predictive ADAM9 transcript, which encodes a shorter form of ADAM9 that lacks the transmembrane and cytoplasmic domains (31). This transcript shares all 19 exons found in transmembrane form, except for 1 additional exon, designated exon 12, which is absent in the transcript that encodes the transmembrane form. However, Northern blot analysis revealed the presence of a single band of 4.1 kb (data not shown). By reverse transcription-PCR (RT-PCR) analysis, we detected the presence of exon 12 in activated human HSCs (Fig. 3*C*). PCR-amplified exon 12 products were purified, subcloned, and verified by sequencing to reveal that this exon has 122 bp that encode 9 amino acids not present in the transmembrane form of ADAM9 (ADAM9-L) and, in addition, inserts a TGA stop codon. The PCR analysis also revealed a smaller fragment lacking the 122-bp exon 12, further evidence of the presence of an ADAM9-L transcript in activated HSCs (Fig. 3*B* and *C*). Thus, activated HSCs express both the transmembrane ADAM9-L protein and the alternatively spliced secreted soluble variant, ADAM9-S.

ADAM9-S promotes invasion. To further investigate the ability of ADAM9-S to promote invasion, we did Matrigel assays using purified ADAM9-S. 1,10-Phenanthroline, a metalloprotease inhibitor, strongly inhibited ADAM9-S-induced Matrigel invasion of clone A cells compared with control-treated cells, suggesting a role for the metalloprotease activity of ADAM9-S in invasion (Fig. 4*A*). To assess whether the metalloprotease domain of the purified ADAM9-S was catalytically active, we did gelatin zymography using purified ADAM9-S. A gelatinolytic band migrating at 55 kDa was detected (Fig. 4*B*). This 55-kDa band was confirmed to be ADAM9-S by parallel immunoblot analysis (data not shown). Immunodepletion of ADAM9-S as well as treatment with 1,10-phenanthroline completely blocked gelatinolytic activity, thus confirming that ADAM9-S isolated from HSCs functions as a protease (Fig. 4*B*). It is worth noting that 1,10-phenanthroline is a broad-range metalloprotease inhibitor, so it is formally possible that the effects observed here could be due to inhibition of other ADAMs or even other matrix metalloproteases.

ADAM9-S cDNA was cloned by RT-PCR amplification from mRNA isolated from activated human HSCs. A 1725 bp product was obtained corresponding to an open reading frame of 575 amino acids. Myc-tagged ADAM9-S was transiently expressed in HeLa cells to verify expression. Immunoblotting of the transfected cells with anti-Myc revealed expression of a 55-kDa protein in both total cell lysate and culture medium (data not shown). To further evaluate whether ADAM9-S cloned from activated HSC encodes a functional protein capable of promoting invasion, Matrigel assays were carried out in Caco-2 cells, a noninvasive

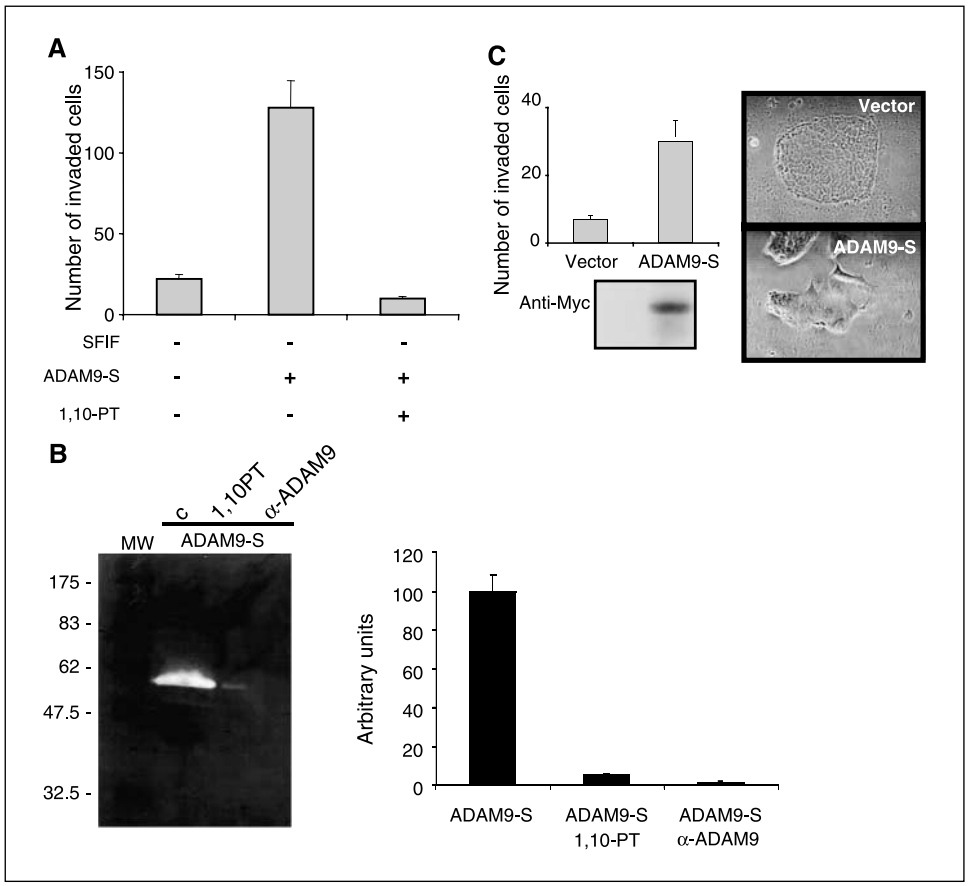

Figure 4. ADAM9-S promotes invasion. *A,* Matrigel invasion of clone A carcinoma cells in the presence of soluble ADAM9-S (20 μg/mL) either alone or in the presence of 1,10-phenanthroline (*1,10-PT*), SFIF, or control. *B,* zymography profile of the protease activity of soluble ADAM9-S either alone or in the presence of 100 μmol/L 1,10-phenanthroline or immunodepletion with anti-ADAM9 (*left*). Densitometric quantification of bands (*right*). *C,* Caco-2 colon cancer cells were transiently transfected with ADAM9-S or vector control, and after transfection, cells were assayed for Matrigel invasion. Also shown is the morphology of cells 24 hours after transfection (*right*, magnification, ×100) and the expression of ADAM9-S in total lysates (*bottom*, anti-Myc immunoblotting). All experiments were carried out in triplicate. *Bars,* SD.

colon cancer cell line that does not express endogenous ADAM9-S. We observed a 5-fold increase in Matrigel invasion in Caco-2 cells transiently expressing ADAM9-S compared with control transfected cells (Fig. 4*C*). A change in cell morphology of the transfected cells was also observed, consistent with a more aggressive motile phenotype.

ADAM9-S promotes carcinoma cell invasion through the binding of laminin receptors. It has been shown that the integrins $\alpha_6\beta_4$ and $\alpha_2\beta_1$ function as laminin-1 receptors in clone A colon carcinoma cells and mediate cell migration through laminin-1 (32, 33). We therefore evaluated whether ADAM9-S could interact with these integrins and influence invasion. Cells were first preincubated with human recombinant ADAM9-S and then allowed to interact with distinct anti-integrin antibodies. ADAM9-S was able to decrease the binding of anti-α_2, anti-α_6, anti-β_1, and anti-β_4 antibodies to these integrin subunits in clone A cells, indicating that ADAM9-S competes for binding to integrins (Supplementary Fig. S2). We also did quantitative adhesion assays on wells coated with recombinant ADAM9-S using clone A cells preincubated with specific anti-integrin antibodies. Preincubation with antibodies to α_2, α_6, β_1, and β_4 integrins significantly reduced clone A cell adhesion to recombinant ADAM9-S, whereas no effect was observed on adhesion to α_3, α_5, and control IgG (Fig. 5*A*). Coimmunoprecipitation experiments also revealed binding of recombinant ADAM9-S to integrin α_2, α_6, β_1, and β_4 subunits but not to α_3 or α_5 subunits (Fig. 5*B*). Finally, we determined whether the binding of ADAM9-S to $\alpha_6\beta_4$ and $\alpha_2\beta_1$ is functionally relevant for invasion. ADAM9-S stimulated invasion through laminin-1 when cells were treated with control IgG; however, both basal invasion and ADAM9-S-stimulated invasion were strongly attenuated in the presence of function-blocking integrin antibodies (Fig. 5*C*). Therefore, the interaction of ADAM9-S with $\alpha_6\beta_4$ and $\alpha_2\beta_1$ is required for invasion through laminin.

To further show that ADAM9-S is catalytically active against laminin, laminin gel zymography was done. A laminin lytic band was detected in the zymogram and shown to be ADAM9-S by immunoblot analysis (Fig. 6*A*; data not shown). As expected, 1,10-phenanthroline inhibited the laminin lytic activity of ADAM9-S. Moreover, a synthetic peptide, which mimics the ADAM9-S disintegrin loop (GKTSECDVPE), potently blocked invasion of clone A cells expressing ADAM9-S when compared with control peptide (Fig. 6*B*). Finally, when clone A cells expressing ADAM9-S were preincubated with the disintegrin loop peptide, there was a significantly impaired attachment of cells to laminin-1, such that most cells showed a round morphology and were not able to spread (Fig. 6*C*).

ADAM9 expression in human liver metastases. To emphasize the relevance of ADAM9 expression in HSCs with respect to invasive disease, we examined the pattern of expression in sections from human liver metastases by immunohistochemistry. A total of 23 specimens of liver metastatic tissue were examined, 19 from colon adenocarcinoma and 4 from uveal melanoma (Fig. 7). Serial sections were also stained against α-SMA to identify HSCs (Fig. 7*A2* and *B2*). Sections were taken from the interface between the tumor and the adjacent liver (junctional specimen). Initial examination revealed that all specimens tested were positive for ADAM9 expression, with a staining pattern almost exclusively confined to the stroma. Closer examination revealed that ADAM9 expression

was most prominent at the invasive front of the metastatic tumor in both colon metastases (Fig. 7*A1* and *A3*) and uveal melanoma metastases (Fig. 7*B1* and *B3*). ADAM9 expression was evident primarily in cells at the tumor-stromal interface, particularly in cells infiltrating the dense fibrous stroma and in tight contact with tumor cells that seemed to be engaged in invasive activity (*solid arrows*; Fig. 7*A3* and *B3*). Moreover, we also detected ADAM9 staining in the stromal cells surrounding the tumor (*open arrows*; Fig. 7*A4* and *B4*). Finally, in all cases, both the tumor cells and the liver hepatocytes were negative for ADAM9 expression (*solid arrows*; Fig. 7*A1* and *B1*).

Discussion

Tumor invasion and metastasis are complex processes with genetic and biochemical determinants that are not completely understood. The two processes share mechanisms that are closely related, because both use similar strategies involving changes in the physical coupling of cells to their microenvironment and activation of extracellular proteases. Here, we report that a soluble form of ADAM9 (designated ADAM9-S) is secreted by activated human HSCs and potently promotes cancer cell invasion.

During tumor progression, changes in the stroma support invasion and metastasis (34, 35). The host stromal component of invasive carcinoma is characterized by an abundance of myofibroblasts, including HSCs in their activated state (5, 36, 37). As part of our screening strategy to identify soluble factors released by activated HSCs, we noticed that the CM of activated human HSCs is endowed with potent invasion-promoting activity toward several cancer cell types, particularly those that preferentially metastasize to the liver. Importantly, CM collected from quiescent, nonactivated HSCs did not promote invasion, indicating that this activity is exerted by liver myofibroblast-like cells in the context of stromal activation induced during tumor invasion (Fig. 8). These results are also in agreement with previous studies that made use of activated rat HSCs, further indicating that this cell type is able to secrete factors that influence cancer cell motility (8, 38). Biochemical and proteomic analyses revealed that one of the soluble factors released by these cells is ADAM9-S.

ADAM9, also known as meltrin γ or metalloprotease disintegrin cysteine-rich protein-9, was originally described by Blobel et al. as an 84-kDa transmembrane cell surface protein (20). Although ADAM9 is generally considered a transmembrane molecule, a secreted form of ADAM9 (ADAM9-S), which displays an α-secretase activity for the amyloid precursor protein, has recently been described (31). In our studies, we found that ADAM9-S is only expressed during the activation of HSCs. Consistent with this notion, we found that ADAM9-S is derived from alternative splicing

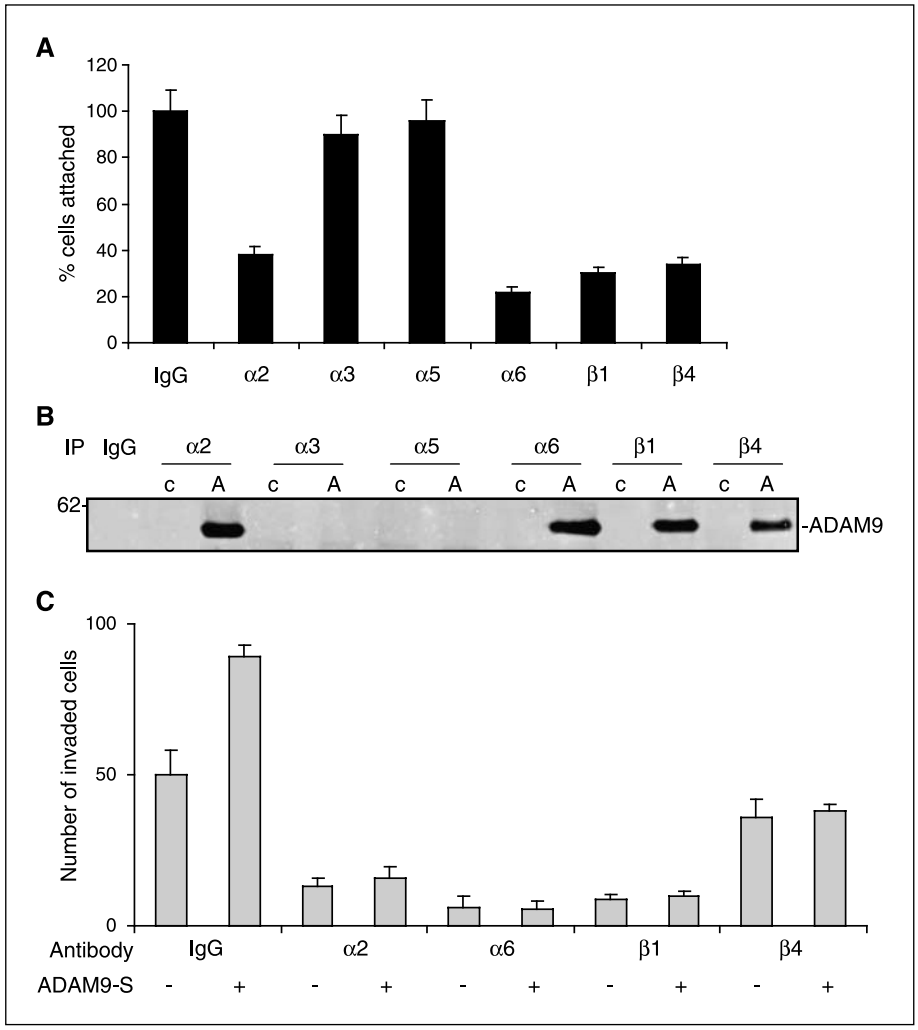

Figure 5. ADAM9-S promotes carcinoma cell invasion by binding to laminin receptors. *A,* clone A cells were resuspended in the presence or absence of blocking mAbs (10 μg/mL) to different integrin subunits before the adhesion assay and then plated on ADAM9-S precoated wells. *B,* clone A cells were incubated with 20 μg/mL soluble recombinant ADAM9-S (*A*) or control buffer (*c*) for 30 minutes and then lysed and integrin subunits were immunoprecipitated using specific antibodies. ADAM9-S was detected by immunoblotting. *C,* clone A cells were incubated for 30 minutes with anti-integrin blocking antibodies (10 μg/mL; α_2: P1E6, α_6: GoH3, β_1: mAb13, and β_4: 3E1) or control IgG followed by a further incubation for 30 minutes with ADAM9-S. Laminin-1 invasion assays were then done. All experiments were carried out in triplicate. *Bars,* SD.

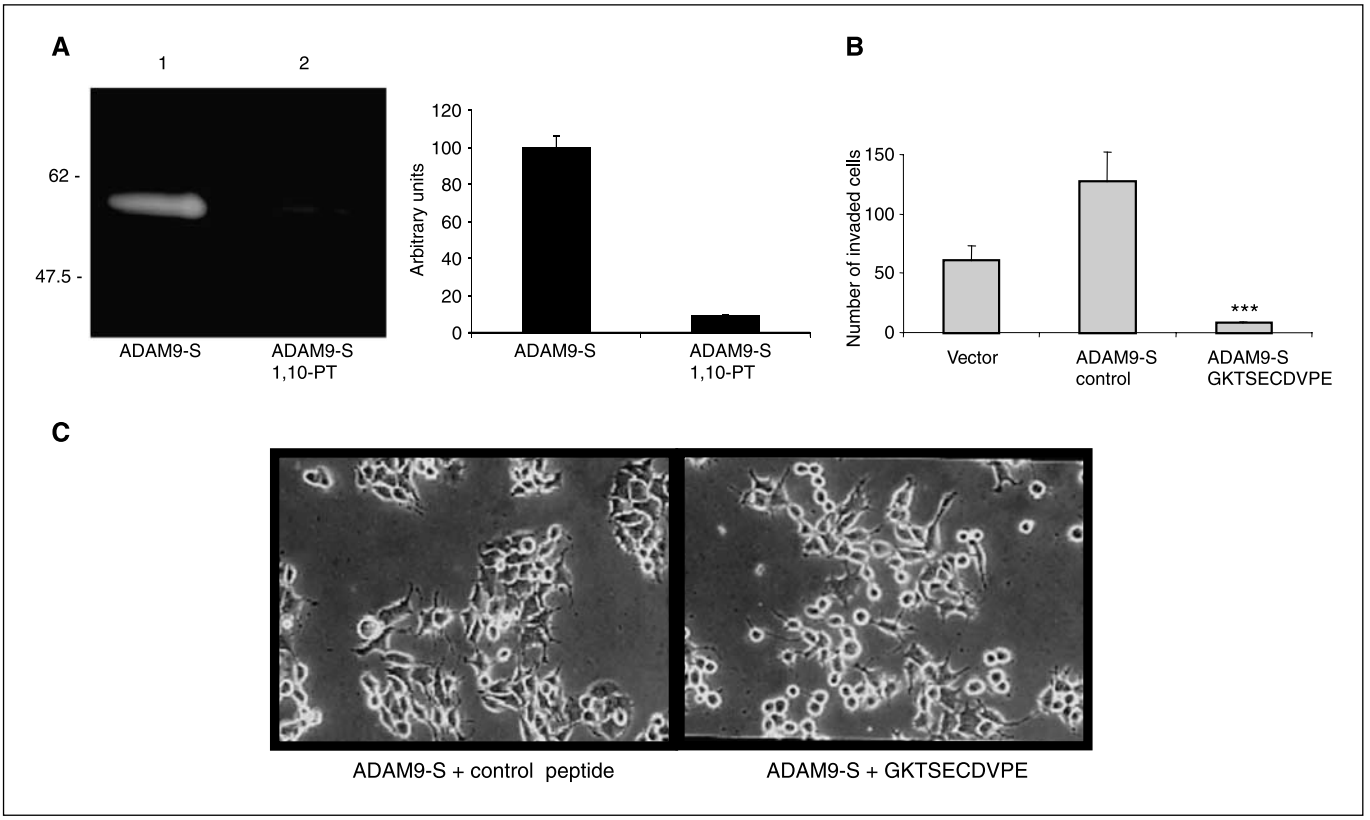

Figure 6. The disintegrin domain of ADAM9-S is required for invasion. *A,* recombinant ADAM9-S (1 μg) was resolved under native conditions and analyzed by laminin gel zymography (*left*). 1,10-Phenantroline (100 μmol/L) was added to the zymograms where indicated. Densitometric quantification (*right*). *B,* clone A cells expressing ADAM9-S were preincubated with 20 μg/mL synthetic peptide GKTSECDVPE or control peptide TLKEDTVCPS and then allowed to invade through laminin-1-coated filters. *C,* analysis of cell morphology of clone A cells expressing ADAM9-S on laminin-1. Twenty-four hours after transfection with ADAM9-S, cells were preincubated with 20 μg/mL synthetic peptide (GKTSECDVPE) or control peptide (TLKEDTVCPS) and then allowed to adhere to laminin-1 precoated dishes. After 1 hour, cells were photographed (magnification, ×100). All experiments were carried out in triplicate. *Bars,* SD. ***, $P < 0.001$.

due to the in-frame insertion of an additional exon, which is absent in the transmembrane ADAM9-L protein. Interestingly, these findings recapitulate previous observations on the human ADAM11 and ADAM12 genes, which are also alternatively spliced and generate two different transcripts, one encoding the transmembrane form and the other a truncated soluble form that lacks the transmembrane and cytoplasmic domains (39, 40).

The functional relevance of ADAM9-S in tumor cell invasion was revealed by the finding that expression of ADAM9-S in noninvasive colon carcinoma cells Caco-2 induced a highly invasive phenotype. This activity was blocked by metalloprotease inhibitors, and because the metalloprotease domain of ADAM9 shows a nonspecific catalytic activity against several substrates, such as gelatin, β-casein, fibronectin, and insulin B-chain (21, 41), it is possible that other domains in ADAM9-S could influence the metalloprotease activity toward specific target membrane receptors presumably required for the invasive process. We reasoned that the ADAM9-S disintegrin domain is a good candidate for such a domain, because several disintegrin domains have been shown to support integrin-mediated cell adhesion (42–44) and also because adhesion to ECM components through integrins is a prerequisite for tumor invasion (1). One of the best understood integrin dimers capable of creating the necessary traction forces required to generate forward movement during colon carcinoma invasion is the laminin receptor $\alpha_6\beta_4$ (45). In addition, $\alpha_2\beta_1$, commonly considered a collagen receptor, is actually employed as a laminin-1 receptor by clone A colon carcinoma cells (46). Consistent with this, we found that ADAM9-S can bind $\alpha_6\beta_4$ and $\alpha_2\beta_1$ integrins that are expressed in clone A colon carcinoma cells, leading to a marked increase in the invasion of these cells through laminin-1. ADAM proteins bind integrins through the disintegrin domain, and a region in the so-called disintegrin loop in ADAMs is responsible for the interaction. All ADAMs, except for ADAM10 and ADAM17, contain a disintegrin loop motif (47). Previous studies have shown that at least 12 members of the ADAM family, including ADAM9, contain a potential XECD integrin-binding motif and that this motif can efficiently inhibit fertilin β/$\alpha_6\beta_1$ interactions, which occur between sperm and egg cells (48, 49). Inhibition of integrin binding to ADAM23 by the disintegrin loop has also been shown (50). Our results are also consistent with an important role for the ADAM9-S disintegrin loop in modulating the interaction with $\alpha_6\beta_4$ and $\alpha_2\beta_1$ integrins.

Finally, we investigated the expression of ADAM9 in surgical specimens obtained during liver resections of hepatic metastases from colon carcinomas and uveal melanomas. These are both tumors that preferentially metastasize to the liver. We found a strong expression of ADAM9 in the stroma and at the invading front of liver metastases, with a clear codistribution with α-SMA-positive stromal cells, likely representing HSCs in their activated state. These findings agree with previous reports describing increased mRNA levels of ADAM9 and ADAM12 in hepatocellular carcinoma and colorectal liver metastases (23). Similarly, expression

of ADAM9 in non–small cell lung cancer has been correlated with brain metastases (24); furthermore, ADAM9 expression in pancreatic cancer has been suggested to be a prognostic factor in ductal adenocarcinoma (51). However, our studies, for the first time, point to the stromal component of an invasive tumor as the source of ADAM9 expression and thus suggest a functional role for stroma-derived ADAM9 in the context of local invasion of metastatic cancer cells. It is important to stress that the expression of ADAM9 was not detected in carcinoma cells or in hepatocytes. The observation that ADAM9 is expressed by α-SMA-positive/activated HSCs in cirrhotic liver tissue further confirms that the expression of this protease is related to the

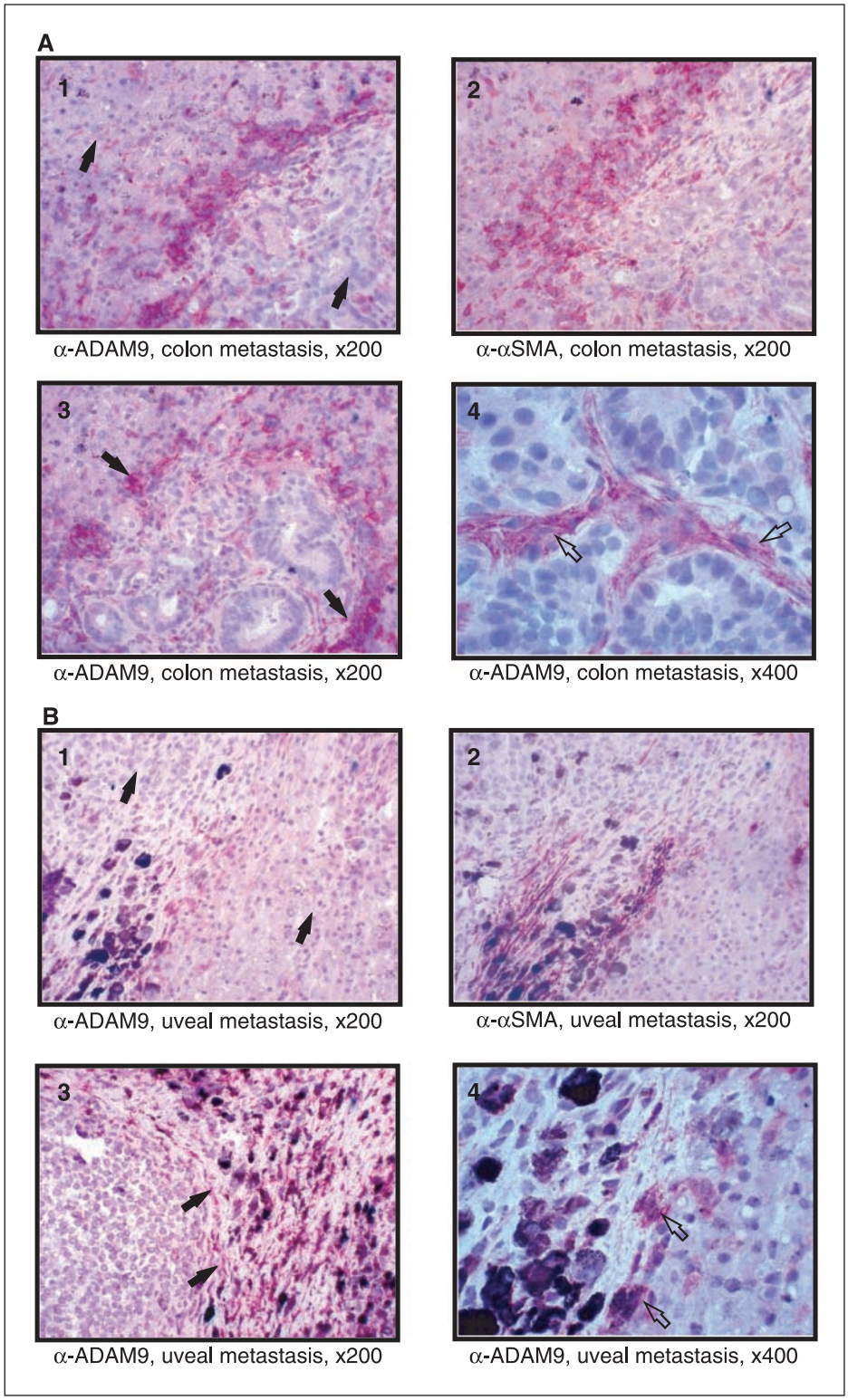

Figure 7. ADAM9 expression in human liver metastatic colon adenocarcinoma and uveal melanoma. Tissue specimens derived from colon carcinoma (*A1-A4*) and uveal melanoma (*B1-B4*) metastasized to the liver were immunostained with anti-ADAM9 (*A1*, *A3*, *A4*, *B1*, *B3*, and *B4*). Serial sections were also stained with anti-α-SMA (*A2* and *B2*). Highlighted are the preferential localization of ADAM9 at the invasive front of metastatic colon carcinoma (*solid arrows*; *A3*) and uveal melanoma (*solid arrows*; *B3*). Expression of ADAM9 in stromal liver HSCs in metastatic colon carcinoma (*open arrows*; *A4*) and uveal melanoma (*open arrows*; *B4*). Absence of ADAM9 expression in hepatocytes and tumor cells of metastatic colon carcinoma (*solid arrows*; *A1*) and uveal melanoma (*solid arrows*; *B1*).

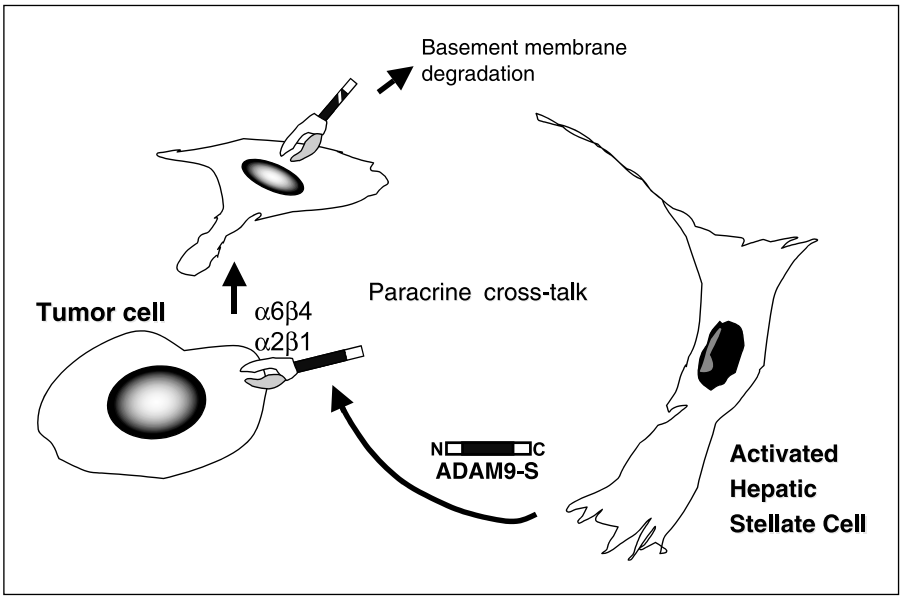

Figure 8. Proposed role of ADAM9-S in promoting invasion through tumor-stromal interactions. Proposed model for the mechanism by which ADAM9-S promotes invasion of cancer cells. Soluble ADAM9-S is released by activated HSCs and binds to $\alpha_6\beta_4$ and $\alpha_2\beta_1$ integrins on the surface of tumor cells. Through its proteolytic activity, ADAM9-S then promotes invasion by degrading components of the basement membrane, including laminin-1, thus allowing tumor cells to invade the surrounding matrix.

activation state of this important component of the hepatic stroma.[5] Although it is tempting to speculate that invading cancer cells secrete soluble factors that influence the activation of HSCs (8, 37), it is also well established that any perturbation of the perisinusoidal microenvironment, which likely occurs during cancer cell extravasation, leads to HSC activation (52, 53). It should also be noted that the expression patterns reveled in our study did not discern between the transmembrane ADAM9-L and the soluble ADAM9-S variants, because the epitope for the ADAM9 antibody is shared by both forms. Future studies with specific antibodies, which can distinguish between ADAM9-L and ADAM9-S, may reveal further distinctions, but regardless, the present data point to an important role for this ADAM family member in modulating tumor-stromal interactions at sites of tumor invasion.

In conclusion, the present study supports a role for liver stromal cells, particularly activated HSCs, in modulating invasion through secretion of ADAM9-S. We propose a model in which ADAM9-S produced by activated HSCs acts in a paracrine fashion on liver metastatic carcinoma cells through interactions with integrin receptors for laminin. In this model, ADAM9-S would be localized in a proteolytically active form proximal to the cell surface of invasive cells and could regulate both laminin degradation and cell motility, thereby facilitating invasion (Fig. 8). Further studies are now required to explore the function of ADAM9-S in liver metastasis *in vivo*. Exploration of ADAM9 expression and function in other invasive tumors, particularly in the stromal component, may further point to an essential role for this protein in modulating tumor-stromal interactions. The data presented in this study may also provide novel insights for designing more effective strategies aimed at preventing the development of hepatic metastasis.

[5] A. Mazzocca and A. Toker, unpublished data.

Acknowledgments

Received 12/19/2004; revised 2/24/2005; accepted 3/16/2005.

Grant support: NIH grants CA96710 (A. Toker) and DK58739 (T.A. Libermann) and Associazione Italiana per la Ricerca sul Cancro (M. Pinzani).

The costs of publication of this article were defrayed in part by the payment of page charges. This article must therefore be hereby marked *advertisement* in accordance with 18 U.S.C. Section 1734 solely to indicate this fact.

We thank Bruce Ksander for kindly providing the OMM2.3 cells and the members of the Toker laboratory for technical assistance and insightful discussions.

References

1. Friedl P, Wolf K. Tumour-cell invasion and migration: diversity and escape mechanisms. Nat Rev Cancer 2003;3:362–74.
2. Liotta LA, Kohn EC. The microenvironment of the tumour-host interface. Nature 2001;411:375–9.
3. Kavolius J, Fong Y, Blumgart LH. Surgical resection of metastatic liver tumors. Surg Oncol Clin N Am 1996;5:337–52.
4. Fidler IJ. The organ microenvironment and cancer metastasis. Differentiation 2002;70:498–505.
5. Ooi LP, Crawford DH, Gotley DC, et al. Evidence that "myofibroblast-like" cells are the cellular source of capsular collagen in hepatocellular carcinoma. J Hepatol 1997;26:798–807.
6. Lunevicius R, Nakanishi H, Ito S, et al. Clinicopathological significance of fibrotic capsule formation around liver metastasis from colorectal cancer. J Cancer Res Clin Oncol 2001;127:193–9.
7. Reeves HL, Friedman SL. Activation of hepatic stellate cells—a key issue in liver fibrosis. Front Biosci 2002;7:d808–26.
8. Olaso E, Santisteban A, Bidaurrazaga J, Gressner AM, Rosenbaum J, Vidal-Vanaclocha F. Tumor-dependent activation of rodent hepatic stellate cells during experimental melanoma metastasis. Hepatology 1997;26:634–42.
9. Lynch CC, Matrisian LM. Matrix metalloproteinases in tumor-host cell communication. Differentiation 2002;70:561–73.
10. DeClerck YA. Interactions between tumour cells and stromal cells and proteolytic modification of the extracellular matrix by metalloproteinases in cancer. Eur J Cancer 2000;36:1258–68.
11. Basset P, Bellocq JP, Wolf C, et al. A novel metalloproteinase gene specifically expressed in stromal cells of breast carcinomas. Nature 1990;348:699–704.
12. Sternlicht MD, Lochter A, Sympson CJ, et al. The stromal proteinase MMP3/stromelysin-1 promotes mammary carcinogenesis. Cell 1999;98:137–46.
13. Nelson AR, Fingleton B, Rothenberg ML, Matrisian LM. Matrix metalloproteinases: biologic activity and clinical implications. J Clin Oncol 2000;18:1135–49.
14. Coussens LM, Tinkle CL, Hanahan D, Werb Z. MMP-9 supplied by bone marrow-derived cells contributes to skin carcinogenesis. Cell 2000;103:481–90.
15. Seals DF, Courtneidge SA. The ADAMs family of metalloproteases: multidomain proteins with multiple functions. Genes Dev 2003;17:7–30.
16. Black RA, White JM. ADAMs: focus on the protease domain. Curr Opin Cell Biol 1998;10:654–9.
17. Zhang XP, Kamata T, Yokoyama K, Puzon-McLaughlin W, Takada Y. Specific interaction of the

recombinant disintegrin-like domain of MDC-15 (metargidin, ADAM-15) with integrin $\alpha_v\beta_3$. J Biol Chem 1998;273:7345–50.
18. Iba K, Albrechtsen R, Gilpin BJ, Loechel F, Wewer UM. Cysteine-rich domain of human ADAM 12 (meltrin α) supports tumor cell adhesion. Am J Pathol 1999; 154:1489–501.
19. Nath D, Slocombe PM, Webster A, Stephens PE, Docherty AJ, Murphy G. Meltrin γ (ADAM-9) mediates cellular adhesion through α(6)β(1) integrin, leading to a marked induction of fibroblast cell motility. J Cell Sci 2000;113:2319–28.
20. Weskamp G, Kratzschmar J, Reid MS, Blobel CP. MDC9, a widely expressed cellular disintegrin containing cytoplasmic SH3 ligand domains. J Cell Biol 1996; 132:717–26.
21. Schwettmann L, Tschesche H. Cloning and expression in *Pichia pastoris* of metalloprotease domain of ADAM 9 catalytically active against fibronectin. Protein Expr Purif 2001;21:65–70.
22. O'Shea C, McKie N, Buggy Y, et al. Expression of ADAM-9 mRNA and protein in human breast cancer. Int J Cancer 2003;105:754–61.
23. Le Pabic H, Bonnier D, Wewer UM, et al. ADAM12 in human liver cancers: TGF-β-regulated expression in stellate cells is associated with matrix remodeling. Hepatology 2003;37:1056–66.
24. Shintani Y, Higashiyama S, Ohta M, et al. Overexpression of ADAM9 in non-small cell lung cancer correlates with brain metastasis. Cancer Res 2004;64: 4190–6.
25. Casini A, Pinzani M, Milani S, et al. Regulation of extracellular matrix synthesis by transforming growth factor β1 in human fat-storing cells. Gastroenterology 1993;105:245–53.
26. Albini A, Iwamoto Y, Kleinman HK, et al. A rapid *in vitro* assay for quantitating the invasive potential of tumor cells. Cancer Res 1987;47:3239–45.
27. Kleiner DE, Stetler-Stevenson WG. Quantitative zymography: detection of picogram quantities of gelatinases. Anal Biochem 1994;218:325–9.
28. Milani S, Grappone C, Pellegrini G, et al. Undulin RNA and protein expression in normal and fibrotic human liver. Hepatology 1994;20:908–16.
29. Verschueren H, Van der Taelen I, Dewit J, De Braekeleer J, De Baetselier P. Metastatic competence of BW5147 T-lymphoma cell lines is correlated with *in vitro* invasiveness, motility and F-actin content. J Leukoc Biol 1994;55:552–6.
30. Kerlavage A, Bonazzi V, di Tommaso M, et al. The Celera discovery system. Nucleic Acids Res 2002;30: 129–36.
31. Hotoda N, Koike H, Sasagawa N, Ishiura S. A secreted form of human ADAM9 has an α-secretase activity for APP. Biochem Biophys Res Commun 2002;293:800–5.
32. Chao C, Lotz MM, Clarke AC, Mercurio AM. A function for the integrin $\alpha_6\beta_4$ in the invasive properties of colorectal carcinoma cells. Cancer Res 1996;56: 4811–9.
33. Rabinovitz I, Mercurio AM. The integrin $\alpha_6\beta_4$ functions in carcinoma cell migration on laminin-1 by mediating the formation and stabilization of actin-containing motility structures. J Cell Biol 1997;139: 1873–84.
34. Wernert N. The multiple roles of tumour stroma. Virchows Arch 1997;430:433–43.
35. De Wever O, Mareel M. Role of tissue stroma in cancer cell invasion. J Pathol 2003;200:429–47.
36. De Wever O, Mareel M. Role of myofibroblasts at the invasion front. Biol Chem 2002;383:55–67.
37. Desmouliere A, Guyot C, Gabbiani G. The stroma reaction myofibroblast: a key player in the control of tumor cell behavior. Int J Dev Biol 2004;48:509–17.
38. Shimizu S, Yamada N, Sawada T, et al. *In vivo* and *in vitro* interactions between human colon carcinoma cells and hepatic stellate cells. Jpn J Cancer Res 2000; 91:1285–95.
39. Katagiri T, Harada Y, Emi M, Nakamura Y. Human metalloprotease/disintegrin-like (MDC) gene: exon-intron organization and alternative splicing. Cytogenet Cell Genet 1995;68:39–44.
40. Gilpin BJ, Loechel F, Mattei MG, Engvall E, Albrechtsen R, Wewer UM. A novel, secreted form of human ADAM 12 (meltrin α) provokes myogenesis *in vivo*. J Biol Chem 1998;273:157–66.
41. Roghani M, Becherer JD, Moss ML, et al. Metalloprotease-disintegrin MDC9: intracellular maturation and catalytic activity. J Biol Chem 1999;274:3531–40.
42. Zhou M, Graham R, Russell G, Croucher PI. MDC-9 (ADAM-9/meltrin γ) functions as an adhesion molecule by binding the α(v)β(5) integrin. Biochem Biophys Res Commun 2001;280:574–80.
43. Mahimkar R, Visaya O, Pollock AS, Lovett DH. The disintegrin domain of ADAM9: a ligand for multiple β_1 renal integrins. Biochem J 2005;385:461-8.
44. Zhao Z, Gruszczynska-Biegala J, Cheuvront T, et al. Interaction of the disintegrin and cysteine-rich domains of ADAM12 with integrin $\alpha_7\beta_1$. Exp Cell Res 2004;298: 28–37.
45. Rabinovitz I, Gipson IK, Mercurio AM. Traction forces mediated by $\alpha_6\beta_4$ integrin: implications for basement membrane organization and tumor invasion. Mol Biol Cell 2001;12:4030–43.
46. Lotz MM, Korzelius CA, Mercurio AM. Human colon carcinoma cells use multiple receptors to adhere to laminin: involvement of $\alpha_6\beta_4$ and $\alpha_2\beta_1$ integrins. Cell Regul 1990;1:249–57.
47. Wolfsberg TG, White JM. ADAMs in fertilization and development. Dev Biol 1996;180:389–401.
48. Gichuhi PM, Ford WC, Hall L. Evidence that peptides derived from the disintegrin domain of primate fertilin and containing the ECD motif block the binding of human spermatozoa to the zona-free hamster oocyte. Int J Androl 1997;20:165–70.
49. Chen H, Sampson NS. Mediation of sperm-egg fusion: evidence that mouse egg $\alpha_6\beta_1$ integrin is the receptor for sperm fertilin β. Chem Biol 1999;6:1–10.
50. Cal S, Freije JM, Lopez JM, Takada Y, Lopez-Otin C. ADAM 23/MDC3, a human disintegrin that promotes cell adhesion via interaction with the $\alpha_v\beta_3$ integrin through an RGD-independent mechanism. Mol Biol Cell 2000;11:1457–69.
51. Grutzmann R, Luttges J, Sipos B, et al. ADAM9 expression in pancreatic cancer is associated with tumour type and is a prognostic factor in ductal adenocarcinoma. Br J Cancer 2004;90:1053–8.
52. Friedman SL. Molecular regulation of hepatic fibrosis, an integrated cellular response to tissue injury. J Biol Chem 2000;275:2247–50.
53. Pinzani M, Rombouts K. Liver fibrosis: from the bench to clinical targets. Dig Liver Dis 2004;36: 231–42.